Continuously tunable bandwidth filter in SOI

Piero Orlandi,[1,3,*] Carlo Ferrari,[2] Michael John Strain,[3] Antonio Canciamilla,[2] Francesco Morichetti,[2] Marc Sorel,[2] Paolo Bassi,[1] and Andrea Melloni [2]

[1]*Dipartimento di Elettronica, Informatica e Sistemistica, Università di Bologna, Viale Risorgimento 2, Bologna 40136, Italy*
[2]*Dipartimento di Elettronica e Informazione, Politecnico di Milano, Via Ponzio 34/5, Milano 20133, Italy*
[3]*School of Engineering, University of Glasgow, Glasgow G12 8LP, United Kingdom*
**Corresponding author: piero.orlandi@unibo.it*

Received Month X, XXXX; revised Month X, XXXX; accepted Month X, XXXX; posted Month X, XXXX (Doc. ID XXXXX); published Month X, XXXX

We present the design and the fabrication of compact tunable silicon-on-insulator bandpass filters. Based on the integration of a Mach-Zehnder interferometer with ring resonators and activated via thermo-optic controlled phase shifters. The proposed architecture provides wide filter bandwidth tunability from 10% to 90% of the free spectral range preserving the filter off band rejection. © XXXX Optical Society of America

OCIS Codes: 130.7408, 250.5300

Reconfigurable or even programmable photonic integrated devices are fundamental building blocks for the development of highly functional circuits to meet the flexibility requirements of the next generation telecom networks [1-4]. In this scenario integrated optical filters that can be widely tuned in both bandwidth and central wavelength play a key role for example in the implementation of the gridless paradigm in wavelength division multiplexing systems.

Only a few geometries that realize this task have been presented so far, since wide bandwidth tunability cannot be easily obtained whilst maintaining good off-band rejection. Solutions based on the tunability of a single ring resonator (RR) coupling sections [5,6] offer in general limited bandwidth variation range and poor off-band rejection. Filters combining a Mach-Zehnder Interferometer (MZI) with RRs have also been presented [7]. Despite their high off-band rejection performance, the bandwidth tuning range is severely limited due to in-band ripples and insertion loss. A single unbalanced MZI with all-pass RRs can offer instead design flexibility, bandwidth tunability, high off-band rejection and simple control [8].

In this letter we propose and demonstrate a simpler geometry, where only one arm of the MZI is loaded with two RRs cascaded in all-pass configuration. This approach requires only tuning of the RRs and of the MZI unloaded arm phases. It provides wider bandwidth reconfiguration range, easier management with reduced power consumption and central wavelength tunability over the full Free Spectral Range (FSR) at the price of a modest off-band rejection reduction. Results also show the reliability of circuit design [9] based on an optimized fabrication process [10] for the silicon-on-insulator (SOI) platform.

Fig. 1 shows (a) a sketch of the proposed geometry with its relevant design parameters and (b) an optical microscope photograph of a tunable filter designed to exhibit a FSR of 200 GHz. The device is based on an unbalanced MZI with input and output power splitting ratio K_C. One arm of the MZI is loaded with two RRs each with geometric cavity length L_R and power coupling

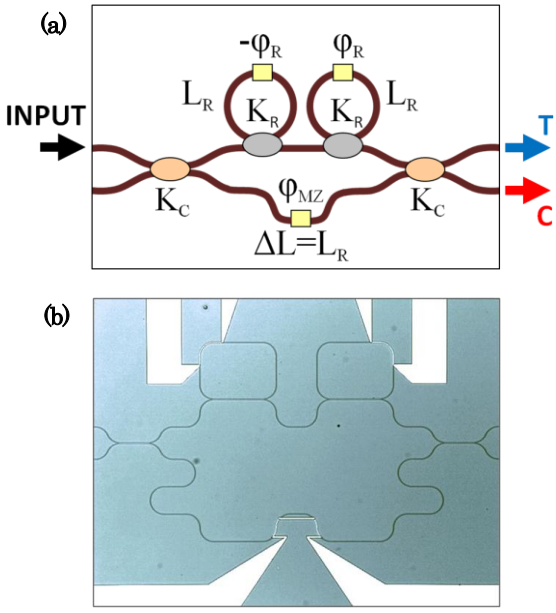

Fig. 1. (a) Filter scheme with relevant design parameters. (b) 200 GHz FSR filter optical microscope photograph.

coefficient K_R. The two S-shaped sections of the unloaded MZI arm (see Fig. 1(b)) are designed to make the path length difference between the two arms of the MZI ΔL equal to L_R (Fig. 1(a)). Under this condition the ring FSR matches that of the MZI. Bandwidth tunability is achieved controlling the phase shift φ_R, antisymmetrically applied to the two RRs. The whole tuning range can be scanned varying $\Delta\varphi = \varphi_R - (-\varphi_R) = 2\varphi_R$ from 0 to 2π. In addition, the filter central wavelength can be tuned over the whole FSR changing the phase of the unloaded MZI arm by φ_r and varying at the same time the RRs phases by the same amount to allow rigid bandwidth translation, since $\Delta\varphi = (\varphi_R + \varphi_{MZ}) - (-\varphi_R + \varphi_{MZ}) = 2\varphi_r$.

The presented geometry was exploited to fabricate a set of devices with different FSR (200, 100 and 25 GHz) on a SOI platform with 220nm thick core layer on a 2μm buried oxide under-cladding. The waveguides were designed for single mode operation, with a width of 480nm, and bend radii of 20μm. These design parameters

ensure respectively low bending losses and compact device footprint size (i.e. always less than 0.6 mm^2). The structure was fabricated using electron-beam lithography into a negative tone Hydrogen Silsequioxane resist that subsequently acted as a hard mask for inductively coupled plasma etching. The silicon waveguides were terminated using polymer mode-converters in order to minimize coupling losses to fiber and facet reflections. Finally, the waveguides were coated with an upper cladding of SiO_2 and the thermo-optic heaters were deposited as a NiCr/Au layer on top [10].

Filter design and analysis has been carried out through circuital simulations performed with a commercial simulation tool [12]. Choosing K_C values equal to 50% provides a symmetric behavior between the through port (T) and the cross port (C) spectra in terms of bandwidth tunability range and off-band rejections. The dependence of these figures of merit from K_R can then be better understood through the color map of Fig. 2, obtained for the T port of a 200 GHz FSR filter considering typical propagation losses of 3 dB/cm and 0.06 dB of insertion loss per coupler. The overall map shape shows that the 3dB bandwidth range that one can span reduces increasing the RRs coupling coefficient K_R. However, the colorbar and the contour lines of Fig. 2 suggest that higher K_R values generally improve the off-band rejection over the whole tuning range. Hence the most suitable value of K_R comes from a design trade off.

Experimental results of the filter bandwidth tunining are shown in Fig. 3 for a 200 GHz FSR filter designed with K_R=70%. Curve colors in Fig. 3(a) and 3(b) refer to filter states corresponding to different phase shift configurations. The device was tested by fiber coupling a tunable laser source to the chip input. TE polarized light was obtained using a polarization controller.

Focusing on the T port filter characteristic of Fig. 3(a), minimum bandwidth condition (red trace) is obtained for $\Delta\varphi=0$ and $\varphi_{MZ}=\pi$. In this case the RRs resonate at the same wavelength, while the MZI transmission maxima at the T port coincide with these resonances. The filter shows a 3 dB bandwidth of 23 GHz with an off-band rejection of about 15 dB. In this configuration the maximum bandwidth condition is achieved at the C port (red trace in Fig. 3(b)) since the MZI transmission maxima occur at the same wavelengths of the RRs antiresonance conditions. This leads to an average cross-talk, evaluated over the T

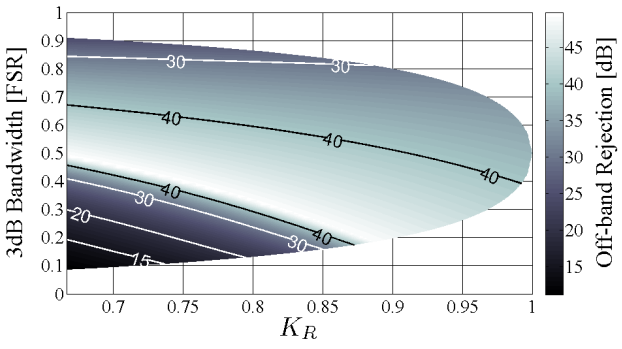

Fig. 2. Through port 3 dB bandwidths obtained varying $\Delta\varphi$ from 0 to 2π (y axis) for different K_R values (x axis) with relative off-band rejection values (color bar and contour lines).

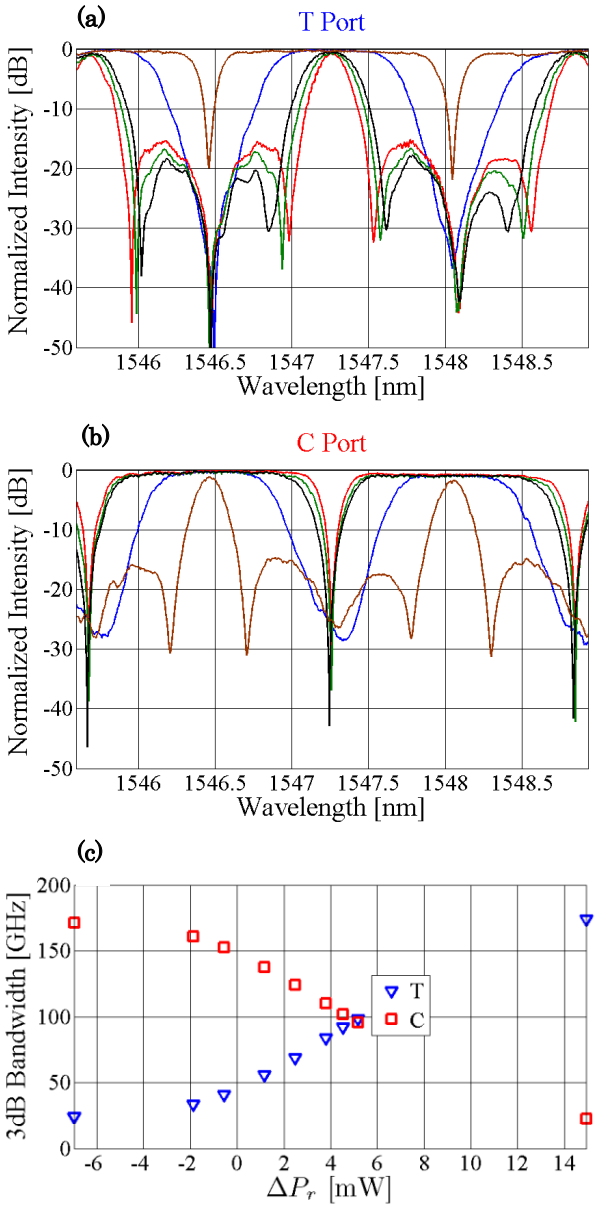

Fig. 3. (Color Line) (a) Bandwidth tuning at the through port and (b) at the cross port for $\Delta\varphi$ that goes from 0 to 2π. (c) 3dB bandwidth achieved for the T port (blue triangles) and the C port (red squares) versus difference between the power dissipated over the two rings ΔP_r.

port 3 dB band, of about -9.4 dB. This filter state, with the RRs resonating together, requires a not equal dissipated power over the two nominally equal rings due to fabrication tolerances [10]: the difference between the dissipated power (ΔP_r) is -7 mW as shown in Fig. 3(c).

To achieve continuous bandwidth tunability, the differential phase shift can then be varied by heating up one of the ring resonators and cooling down the other in a push-pull configuration hence increasing ΔP_r (Fig. 2(c)) and keeping unchanged the power dissipated over the MZI unloaded arm (i.e. ≈ 9 mW in Fig. 2). The maximum bandwidth condition at the T port is achieved when $\Delta\varphi = 2\pi$ (Fig. 2(a) brown trace and Fig. 2(c)). The measured filter 3 dB bandwidth is now 173 GHz with about 20 dB of off-band rejection and 18 dB of average in-band cross-talk.

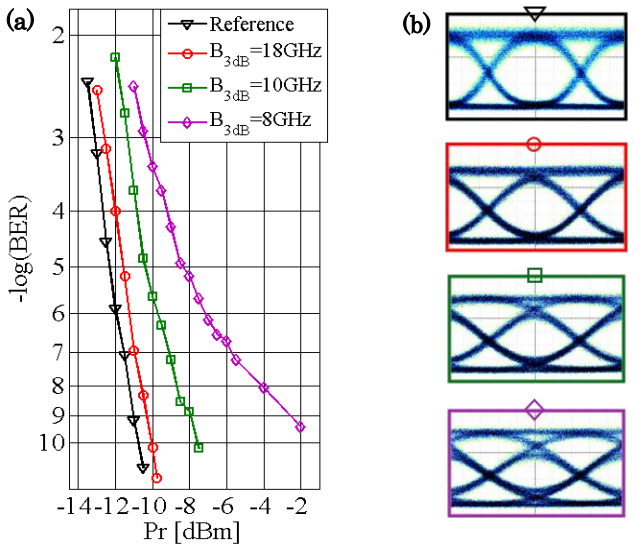

Fig. 4. (Color Line) (a) BER measurements (marks) of a 10 Gbit/sec NRZ OOK filtered by a 200 GHz FSR device with 173 GHz 3 dB bandwidth (black triangles), taken as a reference, and by a 25 GHz FSR device with 3 different 3dB bandwidth: 18 GHz (red circles) 10 GHz (green squares) 8 GHz (magenta diamonds). (b) Relative eye diagrams.

A minimum insertion loss difference between the maximum and the minimum bandwidth of about 0.6 dB has been measured providing almost unchanged penalties over the whole tuning range (Fig. 3(a)). When $\Delta\varphi = \pi$ (crossing point of the curves in Fig. 3(c)) the device acts as a symmetric interleaver, similar to that analyzed in [13]. This condition is close to that shown by the blue trace in Fig. 3(a), Fig. 3(b), where the 3 dB bandwidth at port T is 100 GHz, the extinction ratio is > 30 dB and the in-band average cross-talk is 16.5 dB. From this filter configuration, and in general over the whole tuning range, a not identical behavior between the two ports can be noticed. This asymmetry is caused by unavoidable variations of K_c from the designed 3 dB coupler condition. Despite this non ideality, the device functionality does not vary dramatically (see Fig. 3(a), Fig. 3(b)).

Power consumption for bandwidth tunability is constant (about 28 mW for the device of Fig. 3). It varies only when the central wavelength is tuned. Full wavelength tunability is obtained with 60 mW of variation.

To assess device performances in a realistic scenario, we have then evaluated the Bit Error Rate (BER) of a 10 Gbit/s nonreturn-to-zero (NRZ) on-off keying (OOK) data stream modulated by a $2^7 - 1$ pseudorandom bit sequence and filtered by a 25 GHz FSR tunable filter, with an optical signal-to-noise ratio (OSNR), evaluated over 0.2 nm at the chip input, of 23 dB.

Fig. 4(a) shows that, as expected, the power at the receiver (P_r) needed to reach a determined BER increases reducing the filter bandwidth. The eye diagrams of Fig. 4(b) also show the signal distorsion due to filtering. The eyes are always symmetric, which implies that odd dispersion terms don't affect the signal.

In a scenario were a signal with central wavelength λ_1 needs to be filtered, the filter bandwidth can be adjusted to a value that introduces minimum penalties. If then a signal at λ_2 adjacent to λ_1 is introduced into the system, decreasing the frequency grid spacing, the filter bandwidth can be reduced accordingly at the price of an increase of signal distorsion.

In conclusion, a novel compact filter in Mach-Zehnder configuration with only one arm loaded by ring resonators has been designed by circuital approach and realized in SOI. Wide tunability range, easy management and acceptable off-band rejection have been demonstrated keeping low foot print and low power consumption. Experimental results have shown the consistency of the circuital approach to a SOI platform as well as the robustness against coupler values variation. Moreover, through BER experiments we have shown that the designed filter can be an ideal tool for modern telecom systems based on the gridless paradigm.

Part of this work has been founded by the Italian PRIN 2009 "Shared Access Platform to PHotonic Integrated REsources" (SAPPHIRE) project (http://sapphire.dei.polimi.it/). Authors thank the JWNC staff at Glasgow University for support in fabrication of the devices.

References

1. H. L. R. Lira, C. B. Poitras, and M. Lipson, Opt. Express **19**, 20115–20121 (2011).
2. M. S. Rasras, K.-Y. Tu, D. M. Gill, Y.-K. Chen, A. E. White, S. S. Patel, A. Pomerene, D. Carothers, J. Beattie, M. Beals, J. Michel, and L. C. Kimerling, J. Lightwave Technol. **27**, 2105–2110 (2009).
3. S. Ibrahim, N. K. Fontaine, S. S. Djordjevic, B. Guan, T. Su, S. Cheung, R. P. Scott, A. T. Pomerene, L. L. Seaford, C. M. Hill, S. Danziger, Z. Ding, K. Okamoto, and S. J. B. Yoo, Opt. Express **19**, 13245–13256 (2011).
4. E. Norberg, R. Guzzon, S. Nicholes, J. Parker, and L. Coldren, IEEE Photon. Technol. Lett. **22**, 109–111 (2011).
5. J. Yao and M. C. Wu, Opt. Lett. 34, 2557–2559 (2007).
6. L. Chen, N. Sherwood-Droz, and M. Lipson, Opt. Lett. **32**, 3361–3363 (2007).
7. Y. Ding, M. Pu, L. Liu, J. Xu, C. Peucheret, X. Zhang, D. Huang, and H. Ou, Opt. Express 19, 6462–6470 (2011).
8. M. S. Rasras, D. M. Gill, S. S. Patel, K.-Y. Tu, Y.-K. Chen, A. E. White, A. T. S. Pomerene, D. N. Carothers, M. J. Grove, D. K. Sparacin, J. Michel, M. A. Beals, and L. C. Kimerling, J. Lightwave Technol. **25**, 87–92 (2007).
9. A. Melloni, A. Canciamilla, C. Ferrari, D. Roncelli, and F. Morichetti, in *Information Photonics (IP), 2011 ICO International Conference on* (Ottawa, Canada, 2011), pp. 1–2.
10. A. Canciamilla, M. Torregiani, C. Ferrari, F. Morichetti, R. M. De La Rue, A. Samarelli, M. Sorel, and A. Melloni, J. Opt. **12**, 104008 (2010).
11. M. Gnan, S. Thoms, D. S. Macintyre, R. M. De La Rue, and M. Sorel, Electron. Lett. **44**, 115–116 (2008).
12. Aspic™ – Filarete srl, Italy, http://www.aspicdesign.com; Phoenix BV, The Netherlands, http://www.phoenixbv.com.
13. C. K. Madsen and J. H. Zhao, *Optical Filter Design and Analysis: A Signal Processing Approach* (John Wiley & Sons, inc., New York, NY, 1999).

References

1. H. L. R. Lira, C. B. Poitras, and M. Lipson, "CMOS compatible reconfigurable filter for high bandwidth non-blocking operation," Opt. Express **19**, 20115–20121 (2011).
2. M. S. Rasras, K.-Y. Tu, D. M. Gill, Y.-K. Chen, A. E. White, S. S. Patel, A. Pomerene, D. Carothers, J. Beattie, M. Beals, J. Michel, and L. C. Kimerling, "Demonstration of a Tunable Microwave-Photonic Notch Filter Using Low-Loss Silicon Ring Resonators," J. Lightwave Technol. **27**, 2105–2110 (2009).
3. S. Ibrahim, N. K. Fontaine, S. S. Djordjevic, B. Guan, T. Su, S. Cheung, R. P. Scott, A. T. Pomerene, L. L. Seaford, C. M. Hill, S. Danziger, Z. Ding, K. Okamoto, and S. J. B. Yoo, "Demonstration of a fast-reconfigurable silicon CMOS optical lattice filter," Opt. Express **19**, 13245–13256 (2011).
4. E. Norberg, R. Guzzon, S. Nicholes, J. Parker, and L. Coldren, "Programmable Photonic Lattice Filters in InGaAsP–InP," IEEE Photon. Technol. Lett. **22**, 109–111 (2011).
5. J. Yao and M. C. Wu, "Bandwidth-tunable add-drop filters based on micro-electro-mechanical-system actuated silicon microtoroidal resonators," Opt. Lett. 34, 2557–2559 (2007).
6. L. Chen, N. Sherwood-Droz, and M. Lipson, "Compact bandwidth-tunable microring resonator," Opt. Lett. **32**, 3361–3363 (2007).
7. Y. Ding, M. Pu, L. Liu, J. Xu, C. Peucheret, X. Zhang, D. Huang, and H. Ou, "Bandwidth and wavelength-tunable optical bandpass filter based on silicon microring-MZI structure" Opt. Express 19, 6462–6470 (2011).
8. M. S. Rasras, D. M. Gill, S. S. Patel, K.-Y. Tu, Y.-K. Chen, A. E. White, A. T. S. Pomerene, D. N. Carothers, M. J. Grove, D. K. Sparacin, J. Michel, M. A. Beals, and L. C. Kimerling, "Demonstration of a fourth-order pole-zero optical filter integrated using CMOS processes," J. Lightwave Technol. **25**, 87–92 (2007).
9. A. Melloni, A. Canciamilla, C. Ferrari, D. Roncelli, and F. Morichetti, "A generic design platform for generic photonic foundries," in *Information Photonics (IP), 2011 ICO International Conference on* (Ottawa, Canada, 2011), pp. 1–2.
10. A. Canciamilla, M. Torregiani, C. Ferrari, F. Morichetti, R. M. De La Rue, A. Samarelli, M. Sorel, and A. Melloni, "Silicon coupled-ring resonator structures for slow light applications: potential, imapirments and ultimate limits," J. Opt. **12**, 104008 (2010).
11. M. Gnan, S. Thoms, D. S. Macintyre, R. M. De La Rue, and M. Sorel, "Fabrication of low-loss photonic wires in silicon-on-insulator using hydrogen silsesquioxane electron-beam resist," Electron. Lett. **44**, 115–116 (2008).
12. Aspic™ – Web sites: Filarete srl, Italy, http://www.aspicdesign.com; Phoenix BV, The Netherlands, http://www.phoenixbv.com.
13. C. K. Madsen and J. H. Zhao, *Optical Filter Design and Analysis: A Signal Processing Approach* (John Wiley & Sons, inc., New York, NY, 1999).